Journal of Hazardous Materials 163 (2009) 174–179

Contents lists available at ScienceDirect

Journal of Hazardous Materials

journal homepage: www.elsevier.com/locate/jhazmat

Rapid removal of heavy metal cations and anions from aqueous solutions by an amino-functionalized magnetic nano-adsorbent

Shih-Hung Huang, Dong-Hwang Chen*

Department of Chemical Engineering, National Cheng Kung University, Tainan 701, Taiwan

ARTICLE INFO

Article history:
Received 18 March 2008
Received in revised form 20 June 2008
Accepted 20 June 2008
Available online 27 June 2008

Keywords:
Adsorption
Heavy metal ions
Magnetic nano-adsorbent
Amino-functionalization

ABSTRACT

A novel magnetic nano-adsorbent has been developed by the covalent binding of polyacrylic acid (PAA) on the surface of Fe_3O_4 nanoparticles and the followed amino-functionalization using diethylenetriamine (DETA) via carbodiimide activation. Transmission electron microscopy image showed that the amino-functionalized Fe_3O_4 nanoparticles were quite fine with a mean diameter of 11.2 ± 2.8 nm. X-ray diffraction analysis indicated that the binding process did not result in the phase change of Fe_3O_4. Magnetic measurement revealed they were nearly superparamagnetic with a saturation magnetization of 63.2 emu/g Fe_3O_4. The binding of DETA on the PAA-coated Fe_3O_4 nanoparticles was demonstrated by the analyses of Fourier transform infrared (FTIR) spectroscopy and zeta potential. After amino-functionalization, the isoelectric point of PAA-coated Fe_3O_4 nanoparticles shifted from 2.64 to 4.59. The amino-functionalized magnetic nano-adsorbent shows a quite good capability for the rapid and efficient adsorption of metal cations and anions from aqueous solutions via the chelation or ion exchange mechanisms. The studies on the adsorption of Cu(II) and Cr(VI) ions revealed that both obeyed the Langmuir isotherm equation. The maximum adsorption capacities and Langmuir adsorption constants were 12.43 mg/g and 0.06 L/mg for Cu(II) ions and 11.24 mg/g and 0.0165 L/mg for Cr(VI) ions, respectively.

1. Introduction

Nanotechnology is quickly developing in various fields. In order to meet diverse requirements, many efforts have been made on the nano-engineering of particle surface to tune the bulk properties, tailor the surface properties (e.g., charge density, functionality, reactivity, biocompatibility, stability, and dispersibility), produce hollow nanostructured materials, and create multi-functional composite nanoparticles [1–11].

Magnetic nano-adsorbents are composed of the magnetic cores and polymeric shells. Compared to the traditional adsorbents, they not only can be manipulated or recovered rapidly by an external magnetic field but also possess quite good performance owing to high efficient specific surface area and the absence of internal diffusion resistance. Furthermore, by the choice and chemical modification of polymeric shells, the surface functionality of magnetic nanoparticles can be tailored for various applications in the fields of high-density data storage, ferrofluids, magnetic resonance imaging (MRI), bioseparation, drug delivery, diagnosis, therapy, and immunoassays [10–20].

Recently, we developed a cationic magnetic nano-adsorbent using iron oxide nanoparticles as cores and polyacrylic acid (PAA) as ionic exchange groups [6]. It possessed a high ion-exchange capacity and could recover the positively charged enzymes and basic dyes quite fast and effectively [6,21]. However, it is less effective for the adsorption of polyvalent metal cations and not valid for the adsorption of anionic species. More recently, we further modified the carboxylic groups of PAA using sulfanilic acid. The resultant sulfonated magnetic nano-adsorbent [22] exhibited significantly improved capability for the adsorption of polyvalent metal cations. Unfortunately, it is still invalid for the adsorption of anionic species.

The chelating resins with nitrogen-containing complex ligands have excellent adsorption capability for polyvalent metal cations owing to the strong affinity between the nitrogen atom and metal cations [18,19,23–25]. In addition, they are also capable of adsorbing anionic species after protonation. So, in this work, we attempted to develop a novel magnetic nano-adsorbent for both metal cations and anions by the further amino-functionalization of PAA-coated magnetic nano-adsorbent with diethylenetriamine via carbodiimide activation as illustrated in Fig. 1. The amino-functionalization was recognized by the analyses of Fourier transform infrared (FTIR) spectra and zeta potentials. The product's capability for the adsorption of various metal cations and anions was studied to demonstrate its practicability, particularly with Cu(II) and Cr(VI) ions as cationic

* Corresponding author. Tel.: +886 6 2757575x62680; fax: +886 6 2344496.
E-mail address: chendh@mail.ncku.edu.tw (D.-H. Chen).

0304-3894/$ – see front matter © 2008 Elsevier B.V. All rights reserved.
doi:10.1016/j.jhazmat.2008.06.075

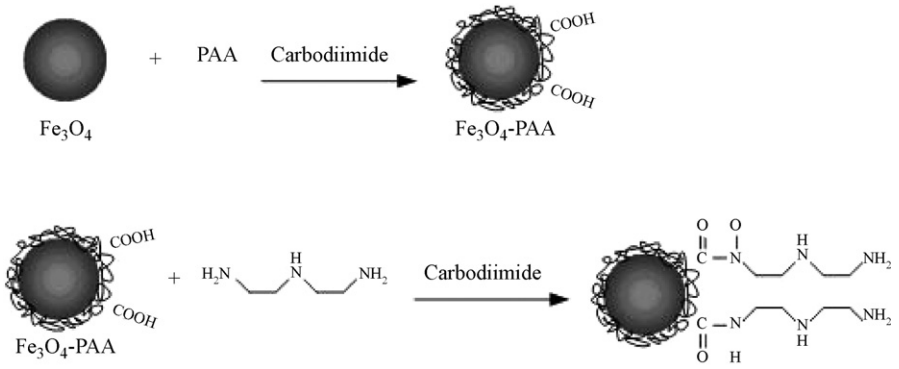

Fig. 1. A scheme for the binding and amino-functionalization of PAA on Fe_3O_4 nanoparticles as a novel magnetic nano-adsorbent for both metal cation and anions.

and anionic model compounds for the investigation on adsorption behavior.

2. Materials and methods

2.1. Materials

Polyacrylic acid solution (25%, degree of polymerization = 2000–3000) and nickel chloride hexahydrate were purchased from Showa Chemical Co. (Tokyo). Carbodiimide was supplied by Sigma Chemical Co. (St. Louis, MO). Ferric chloride hexahydrate was the product of J.T. Baker (Phillipsburg). Ferrous chloride tetrahydrate and chromium(VI) oxide were obtained from Fluka (Buchs). Ammonium hydroxide (29.6%) was supplied by TEDIA (Fairfield). Silver nitrate and cobalt chloride were the products of Mallinckrodt (Paris). Copper(II) nitrate-2,5-hydrate and diethylenetriamine (DETA) were purchased from Riedel-deHaën. Hydrogen tetrachloroaurate(III) trihydrate was supplied by Alfa Aesar (Ward Hill). Palladium(II) chloride was the reagent of E. Merck (Darmstadt). Cadmium chloride anhydrous was obtained from Aros Organics (Belgium). All chemicals were the guaranteed or analytic grade reagents and used without further purification. The water used throughout this work was the reagent-grade water produced by a Milli-Q SP ultra-pure-water purification system of Nihon Millipore Ltd., Tokyo.

2.2. Fabrication and characterization of amino-functionalized magnetic nanoparticles

PAA-coated Fe_3O_4 nanoparticles were prepared according to our previous work [6]. Firstly, Fe_3O_4 nanoparticles were synthesized via the co-precipitation of Fe^{2+} and Fe^{3+} ions (molar ratio 1:2) in an ammonia solution at pH 10, 25 °C and a concentration of 0.3 M iron ions, followed by the hydrothermal treatment at 80 °C for 30 min. Secondly, for the covalently binding of PAA, 100 mg of Fe_3O_4 nanoparticles were mixed with 2 mL of buffer A (0.003 M phosphate, pH 6, 0.1 M NaCl) and 0.5 mL of carbodiimide solution (0.025 g/mL in buffer A). After being sonicated for 10 min, 2.5 mL of PAA solution (60 mg/mL in buffer A) was added and the reaction mixture was sonicated for another 30 min. Finally, the PAA-coated Fe_3O_4 nanoparticles were magnetically recovered and washed with water twice.

For the amino-functionalization of PAA-coated Fe_3O_4 nanoparticles, the above PAA-coated Fe_3O_4 nanoparticles were first mixed with 4.32 mL of buffer A (0.003 M phosphate, pH 6, 0.1 M NaCl) solution and 0.5 mL of carbodiimide solution (0.025 g/mL in buffer A). After being sonicated for 10 min, the reaction mixture was mixed with 0.18 mL of diethylenetriamine (9.1 M) and sonicated for another 60 min. By varying the amount of diethylenetriamine and the volume of buffer A, the concentration of diethylenetriamine was tuned in the range of 0.016–1.62 M and the volume of reaction mixture was fixed at 5 mL. Finally, the magnetic nanoparticles were magnetically recovered and washed with 0.2 M NaOH solution and ethanol, and then dried in a vacuum oven. NaOH was used for the flocculation of magnetic nanoparticles. Its addition could accelerate the magnetic separation. According to the increased weight after PAA binding and amino-functionalization, the amount of amino-functionalized PAA bound on Fe_3O_4 nanoparticles could be estimated to be 3.2 mg/100 mg Fe_3O_4.

The size and morphology of aminated magnetic nanoparticles were observed by transmission electron microscopy (TEM) using a JEOL Model JEM-1200EX at 80 kV. The magnetic measurement was done using a superconducting quantum interference device (SQUID) magnetometer (MPMS7, Quantum Design). X-ray diffraction (XRD) measurement was performed on a Rigaku D/max III.V X-ray diffractometer using Cu Kα radiation (λ = 0.1542 nm). FTIR spectra were recorded on a Thermo Nicolet 320 FTIR spectrometer. Zeta potentials were measured on a Malvern ZEN2600 Zetasizer Nano Z, and before measurement the sample solutions were allowed to equilibrate for 24 h at 25 °C.

2.3. Adsorption studies

The adsorption of various metal cations (Ag^+, Cu^{2+}, Ni^{2+}, Co^{2+}, Cd^{2+}, Fe^{2+}, Fe^{3+}) and anions ($AuCl_4^-$, $PdCl_4^{2-}$, $HCrO_4^-$) by the amino-functionalized magnetic nanoparticles was investigated in aqueous solutions at 25 °C. In general, the amino-functionalized magnetic nanoparticles obtained from 100 mg of Fe_3O_4 nanoparticles were mixed with 5 mL of the corresponding aqueous solution of metal ions (100 mg/L) for 30 min on a shaker to reach the adsorption equilibrium. The concentrations of metal ions were measured using a GBC Avanta Atomic Absorption Spectrometer or the inductively coupled plasma atomic emission spectrometry (Jobin Yvon PA Norama). For comparison, the adsorption of metal cations by the PAA-coated magnetic nanoparticles was also measured. The adsorption behaviors of Cu(II) and Cr(VI) ions by the amino-functionalized magnetic nanoparticles were investigated in aqueous solutions at pH 1–5 and 2–6, respectively. The solution pH was adjusted by NaOH or HCl. The equilibrium isotherms for Cu(II) and Cr(VI) ions at 25 °C were established in aqueous solutions at pH 5 and 2, respectively.

3. Results and discussion

3.1. Determination of diethylenetriamine concentration for amino-functionalization

To determine the appropriate concentration of diethylenetriamine, various amounts of diethylenetriamine (0.016–1.62 M) were used for the amino-functionalization of PAA-coated magnetic nanoparticles at a fixed Fe_3O_4 concentration of 20 mg/mL and a reaction time of 60 min. The amino-functionalization efficiency was estimated by the measurement of products' adsorption capacities for Cu(II) ions at 25 °C, pH 4.6, and an initial concentration of 1000 mg/L. As indicated in Fig. 2, the adsorption capacity of PAA-coated magnetic nanoparticles for Cu(II) ions was significantly enhanced after amino-functionalization with diethylenetriamine. This could be attributed to the fact that PAA-coated magnetic nanoparticles had only monocarboxylic groups whose chelating capability for polyvalent metal cations is weaker than amino groups. Furthermore, because PAA-coated magnetic nanoparticles were negatively charged at pH 4.6 (i.e., isoelectric point ~2.64 [22]), this result also revealed that their adsorption capability for Cu(II) ions via the cation exchange mechanism at this pH value was weaker than that of amino-functionalized magnetic nanoparticles via the chelation mechanism. In addition, the products showed the almost same adsorption capacities for Cu(II) ions when diethylenetriamine concentration was above 0.064 M. Thus, in the following investigations, the diethylenetriamine concentration for the amino-functionalization was fixed at 0.32 M.

3.2. Particle size and structure of amino-functionalized magnetic nanoparticles

The typical TEM image and particle size distribution of the amino-functionalized magnetic nanoparticles were shown in Fig. 3. It was obvious that these particles were quite fine with a mean Fe_3O_4 core diameter of 11.6 ± 2.8 nm. Furthermore, it was notable that the amino-functionalization did not significantly result in the particle agglomeration in spite that diethylenetriamine had two amino groups which might lead to the interparticle crosslinking. This might be due to the use of sufficiently high diethylenetriamine concentration, which led to a higher possibility for the reaction between the carboxylic groups of PAA and the amino groups of unreacted diethylenetriamine.

The XRD patterns of the naked, PAA-coated, and amino-functionalized magnetic nanoparticles indicated six characteristic peaks of Fe_3O_4 at $2\theta = 30.1°$, 35.5°, 43.1°, 53.4°, 57.0° and 62.6°, corresponding to their indices (2 2 0), (3 1 1), (4 0 0), (4 2 2), (5 1 1) and (4 4 0). The magnetic analysis also showed that the saturation magnetization (M_s), remanent magnetization (M_r), coercivity (H_c), and squareness ($S_r = M_r/M_s$) for the naked Fe_3O_4 nanoparticles at 25 °C were 63.2 emu/g, 0.83 emu/g, 8.3 Oe, and 0.013, respectively, and these values for the amino-functionalized ones had no significant changes based on the weight of Fe_3O_4. Both results revealed that the binding and amino-functionalization of PAA did not result in the significant changes in the phase and magnetic property of Fe_3O_4 cores. This could be attributed to the fact that the binding and amino-functionalization of PAA occurred only on the surface of Fe_3O_4 cores.

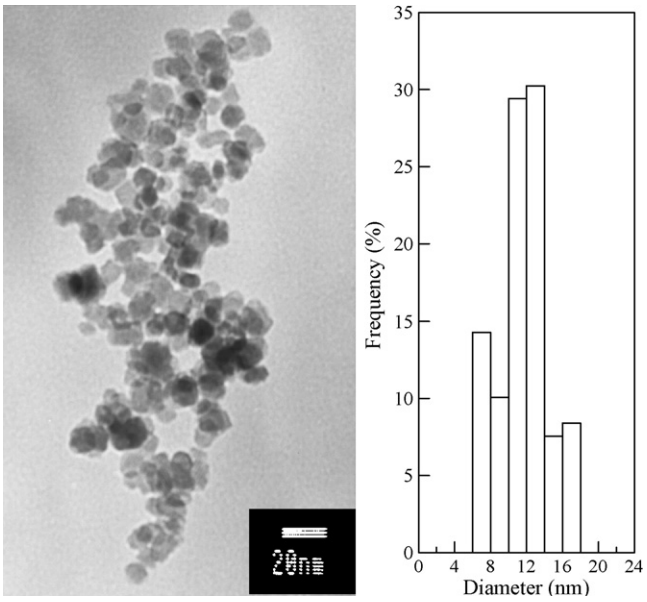

Fig. 3. TEM image and particle size distribution of the amino-functionalized PAA-coated Fe_3O_4 nanoparticles.

3.3. FTIR and zeta potential analyses

Fig. 4 shows the FTIR spectra of PAA-coated and amino-functionalized magnetic nanoparticles. It was observed, after amino-functionalization, that the characteristic peaks of PAA at 1708 cm^{-1} (C=O stretch) 1448 and 1409 cm^{-1} (C—O stretch) disappeared and two new peaks appeared at 1331 cm^{-1} (N—H bend) and 1044 cm^{-1} (C—N stretch). This revealed that the carboxylic

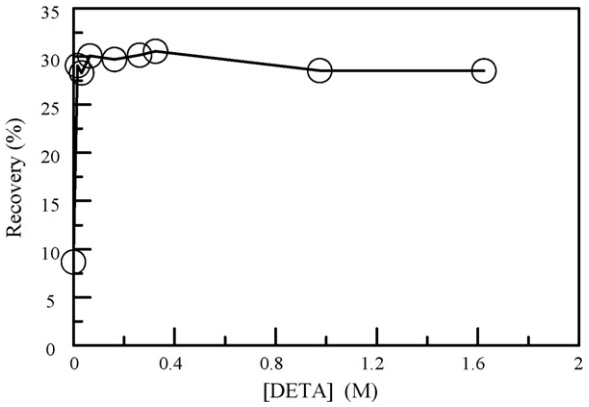

Fig. 2. Effect of DETA concentration on the adsorption of Cu(II) ions at 25 °C, pH 4.6, and an initial concentration of 1000 mg/L. Nanoparticles: 103.2 mg; solution volume: 5 mL.

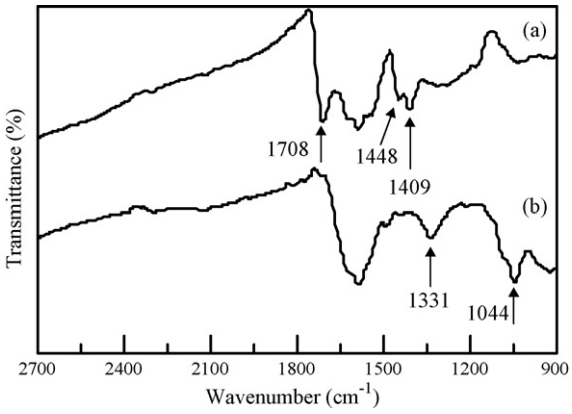

Fig. 4. FTIR spectra of PAA-coated (a) and amino-functionalized (b) Fe_3O_4 nanoparticles.

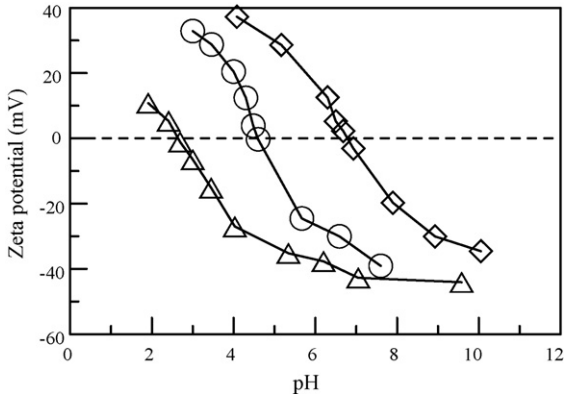

Fig. 5. Zeta potentials of the naked (◊), PAA-coated (△), and amino-functionalized (○) Fe_3O_4 nanoparticles at various pH values. The data for the naked and PAA-coated amino-functionalized Fe_3O_4 nanoparticles were obtained from our previous work [22].

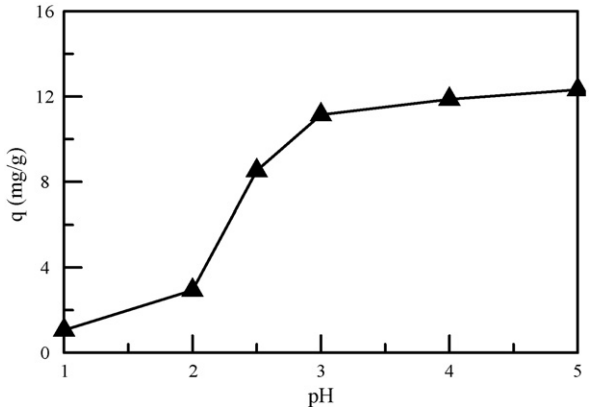

Fig. 6. Effect of pH on the adsorption of Cu(II) ions by the amino-functionalized nanoparticles. Initial concentration of Cu(II) ions: 600 mg/L; nanoparticles: 103.2 mg; solution volume: 5 mL.

acid groups of PAA have been amino-functionalized successfully by reacting with the amino groups of diethylenetriamine.

Since the charge state of carboxylic groups is quite different from that of amino groups, the analysis of zeta potentials was further conducted to confirm the amino-functionalization of PAA-coated magnetic nanoparticles. Fig. 5 indicates the pH-dependences of zeta potentials for the naked, PAA-coated, and amino-functionalized magnetic nanoparticles (100 mg/L) in 0.01 M NaCl solution at pH 1.9–10 (adjusted by NaOH and HCl). The data for the naked and PAA-coated amino-functionalized Fe_3O_4 nanoparticles were obtained from our previous work [22]. It was observed that the isoelectric point (p*I*) of magnetic nanoparticles shifted from 6.78 to 2.64 after PAA binding, and then shifted to 4.59 after further amino-functionalization. This confirmed the amino-functionalization of PAA by diethylenetriamine and revealed that the amino-functionalized magnetic nanoparticles were positively charged at pH < 4.59.

3.4. Adsorption capability

Table 1 demonstrates the feasibility of the amino-functionalized magnetic nanoparticles as a nano-adsorbent for the recovery of both cationic and anionic metal species from aqueous solutions. As compared to the PAA-coated magnetic nanoparticles, the amino-functionalized magnetic nanoparticles exhibited a significantly higher capability of adsorbing mono-, di-, and tri-valent metal cations. Also, they were capable of adsorbing metal anions. Thus, our attempt to develop a novel magnetic nano-adsorbent for both metal cations and anions was achieved. Furthermore, the same measurement for the naked iron oxide nanoparticles has also been done for comparison as indicated in Table 1. In general, the naked iron oxide nanoparticles had weaker adsorption capability than the amino-functionalized magnetic nanoparticles. Moreover, it was noted that the adsorption rates were quite fast and the adsorption equilibria were reached within few minutes for all ionic species examined. This could be reasonably attributed to the absence of internal diffusion resistance.

Table 1
Recovery of various metal cations and anions from aqueous solutions by the naked, PAA-coated, and amino-functionalized magnetic nano-adsorbent

Metal ions	Initial pH	Recovery (%)		
		Naked	PAA-coated	Amino-functionalized
Ag^+	5.83	13.6	41.0	100
Cu^{2+}	5.22	31.7	34.7	~100
Fe^{2+}	4.42	41.3	30.1	98.7
Co^{2+}	5.82	13.9	32.3	~100
Cd^{2+}	5.70	4.2	8.5	100
Ni^{2+}	5.71	12.8	18.6	100
Fe^{3+}	2.51	52.2	82.3	100
$AuCl_4^-$	2.96	~100	–	~100
$PdCl_4^{2-}$	2.61	81.7	–	100
$HCrO_4^-$	2.72	84.6	–	96

Initial concentrations of various metal cations and anions are 100 mg/L. pH values are self-established by the metal salts. Nanoparticles: 103.2 mg; solution volume: 5 mL.

3.5. Adsorption behaviors of Cu(II) and Cr(VI) ions

The effect of solution pH on the adsorption of Cu(II) ions by the amino-functionalized magnetic nanoparticles at 25 °C and an initial Cu(II) ion concentration of 600 mg/L was shown in Fig. 6. It was found that the adsorption capacity increased with increasing solution pH. This revealed the characteristic of chelation mechanism and might be attributed to the less insignificant competitive adsorption of hydrogen ions at higher pH [18,23,25,26]. When pH > 5, no adsorption experiments were conducted because white $Cu(OH)_2$ precipitate was formed.

From the pH dependence, the major characteristic reactions that may take place at the solid-solution interface of amino-functionalized magnetic nanoparticles may be expressed by the following Eqs. (1)–(4) [27,28]:

$$-NH_2 + H^+ = -NH_3^+ \quad (1)$$

$$-NH_2 + Cu^{2+} \rightarrow -NH_2Cu^{2+} \quad (2)$$

$$-NH_2 + OH^- = -NH_2OH^- \quad (3)$$

$$-NH_2OH^- + Cu^{2+}\,(\text{or}\,CuOH^+) = -NH_2OH^-\cdots Cu^{2+}\,(\text{or}\,-NH_2OH^-\cdots CuOH^+) \quad (4)$$

Eq. (1) indicates the protonation and deprotonation reactions of the amino groups of amino-functionalized magnetic nanoparticles in the solution, Eq. (2) represents the formation of surface complexes of Cu^{2+} ion with the amino group, and Eq. (3) describes the adsorption of OH^- ions from the solution through hydrogen bond at high solution pH. At lower solution pH, the reaction in Eq. (1) favored the protonation of $-NH_2$ to form $-NH_3^+$. When more $-NH_2$ groups were converted to $-NH_3^+$, there were only fewer $-NH_2$ sites available on the surface of amino-functionalized magnetic nanoparticles for Cu^{2+} ion adsorption through Eq. (2). Also,

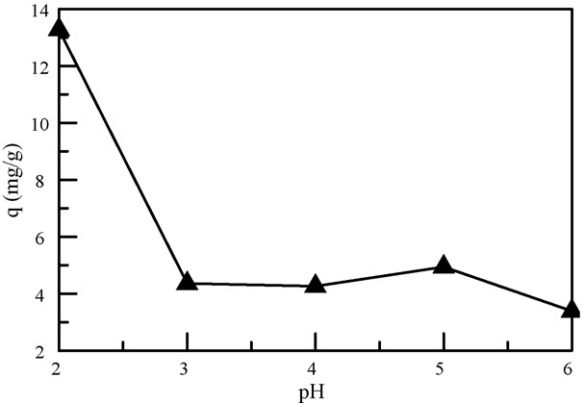

Fig. 7. Effect of pH on the adsorption of Cr(VI) ions by the amino-functionalized nanoparticles. Initial concentration of Cr(VI) ions: 600 mg/L; nanoparticles: 103.2 mg; solution volume: 5 mL.

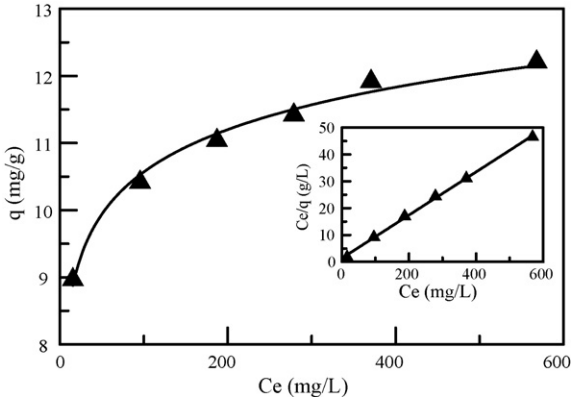

Fig. 8. Equilibrium isotherm for the adsorption of Cu(II) ions on the amino-functionalized nanoparticles at pH 5 and 25 °C. The inset illustrates the linear dependence of C_e/q on C_e. Nanoparticles: 103.2 mg; solution volume: 5 mL.

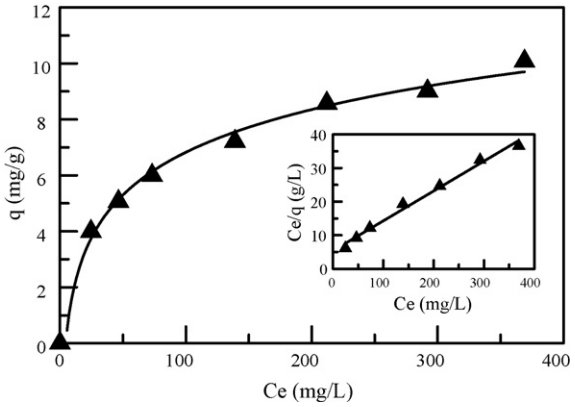

Fig. 9. Equilibrium isotherm for the adsorption of Cr(VI) ions on the amino-functionalized nanoparticles at pH 2 and 25 °C. The inset illustrates the linear dependence of C_e/q on C_e. Nanoparticles: 103.2 mg; solution volume: 5 mL.

the electrostatic repulsion between the Cu^{2+} ions and the surface of amino-functionalized magnetic nanoparticles increased. Both the effects resulted in the reduction of Cu^{2+} ion adsorption on the amino-functionalized magnetic nanoparticles with decreasing solution pH. With increasing solution pH, the reaction in Eq. (1) proceeded to the left, leading to an increase of the number of $-NH_2$ sites on the surface of amino-functionalized magnetic nanoparticles for Cu^{2+} ion adsorption through Eq. (2) and thus increasing the adsorption capacity [28]. At higher solution pH, the reaction in Eq. (3) might proceed, leading to the reduction of Cu^{2+} ion adsorption through surface complexation in Eq. (2). However, the adsorption of Cu^{2+} ions through the electrostatic attraction as indicated in Eq. (4) might increase. This might explain why the increase in the adsorption capacity became slow when pH > 3.

Fig. 7 illustrates the effect of solution pH on the adsorption of Cr(VI) ions by the amino-functionalized magnetic nanoparticles at 25 °C and an initial Cr(VI) ion concentration of 600 mg/L. In contrast to that observed in the case of Cu(II) ions, it was found that higher adsorption capacity was obtained at lower pH. It is known that Cr(VI) ions exists in various anionic forms (i.e., $Cr_2O_7^{2-}$, $HCrO_4^-$, CrO_4^{2-} and $HCr_2O_7^-$) in aqueous solution, depending on the pH and concentration [29]. At lower solution pH, amino groups will be protonated to form $-NH_3^+$ as indicated in Eq. (1) and result in the electrostatic attraction with the negatively charged Cr(VI) ions according to an anionic exchange mechanism [19,29]. The formation of more $-NH_3^+$ groups will increase the number of sites for the binding of Cr(VI) ions. So, the higher adsorption capacity at lower pH for the adsorption of Cr(VI) ions by the amino-functionalized magnetic nanoparticles could be referred to the increased electrostatic attractions between the negatively charged Cr(VI) ions and NH_3^+ groups due to the increased protonation of amino groups.

The equilibrium isotherms for the adsorption of Cu(II) and Cr(VI) ions on the amino-functionalized magnetic nanoparticles were shown in Figs. 8 and 9. The adsorption data were analyzed according to the linear form of Langmuir isotherm as follow [26]:

$$\frac{C_e}{q} = \frac{1}{Kq_m} + \frac{C_e}{q_m} \quad (5)$$

where q is the adsorption capacity (mg/g) based on the dry weight of nano-adsorbent, C_e is the equilibrium concentration (mg/L) in solution, q_m is the maximum adsorption capacity (mg/g) and K is the Langmuir adsorption equilibrium constant (L/mg). As shown in the insets in Figs. 8 and 9, the plots of C_e/q vs. C_e yielded straight lines, revealing that the adsorption of Cu(II) and Cr(VI) ions on the amino-functionalized magnetic nanoparticles obeyed the Langmuir adsorption isotherm. From the slopes and intercepts, the values of q_m and K were calculated to be 12.43 mg/g and 0.06 L/mg for Cu(II) ions and 11.24 mg/g and 0.0165 L/mg for Cr(VI) ions, respectively.

4. Conclusions

A novel magnetic nano-adsorbent has been developed by binding and amino-functionalization of PAA on Fe_3O_4 nanoparticles. TEM, XRD, and magnetic analyses revealed that the structure and magnetic properties of Fe_3O_4 cores were not changed significantly after binding of PAA and amino-functionalization. Also, although diethylenetriamine had two amino groups, no significant particle agglomeration occurred. FTIR analysis indicated the amino-functionalization has been accomplished by the reaction between the carboxylic acid groups of PAA and the amino groups of diethylenetriamine acid via carbodiimide activation. The isoelectric point of PAA-coated magnetic nanoparticles shifted significantly from 2.64 to 4.59 after amino-functionalization. As compared to the PAA-coated magnetic nanoparticles, the amino-functionalized magnetic nanoparticles not only exhibited significantly higher capability of adsorbing mono- and polyvalent metal cations but also became valid for adsorbing the metal anions. Also, the adsorption rate was found to be quite fast and the equilibrium could be achieved within few minutes. In addition, the adsorption of Cu(II) and Cr(VI) ions by the amino-functionalized magnetic nanoparticles revealed the characteristics of chelation and ion-exchange mechanisms, respectively. Also, both followed

the Langmuir isotherm equation with the maximum adsorption capacities and Langmuir adsorption constants of 12.43 mg/g and 0.06 L/mg for Cu(II) ions and 11.24 mg/g and 0.0165 L/mg for Cr(VI) ions, respectively.

Acknowledgements

This work was performed under the auspices of the National Science Council of the Republic of China, under contract number NSC94-2214-E006-006, to which the authors wish to express their thanks.

References

[1] R. Zhang, X. Wang, One step synthesis of multiwalled carbon nanotube/gold nanocomposites for enhancing electrochemical response, Chem. Mater. 19 (2007) 976–978.
[2] S. Ikeda, Y. Ikoma, H. Kobayashi, T. Harada, T. Torimoto, B. Ohtanic, M. Matsumura, Encapsulation of titanium(IV) oxide particles in hollow silica for size-selective photocatalytic reactions, Chem. Commun. (2007) 3753–3755.
[3] T. Gao, Q. Li, T. Wang, Sonochemical synthesis, optical properties, and electrical properties of core/shell-type ZnO nanorod/CdS nanoparticle composites, Chem. Mater. 17 (2005) 887–892.
[4] F. Caruso, Nanoengineering of particle surfaces, Adv. Mater. 13 (2001) 11–22.
[5] C.M. Niemeyer, Nanoparticles, proteins, and nucleic acids: biotechnology meets materials science, Angew. Chem. Int. Ed. 40 (2001) 4128–4158.
[6] M.H. Liao, D.H. Chen, Preparation and characterization of a novel magnetic nano-adsorbent, J. Mater. Chem. 12 (2002) 3654–3659.
[7] M.M. Natile, A. Glisenti, CoO_x/CeO_2 nanocomposite powders: synthesis, characterization, and reactivity, Chem. Mater. 17 (2005) 3403–3414.
[8] S.Y. Yu, H.J. Zhang, J.B. Yu, C. Wang, L.N. Sun, W.D. Shi, Bifunctional magnetic-optical nanocomposites: grafting lanthanide complex onto core–shell magnetic silica nanoarchitecture, Langmuir 23 (2007) 7836–7840.
[9] S. Zhou, B. Varughese, B. Eichhorn, G. Jackson, K. McIlwrath, Pt–Cu core–shell and alloy nanoparticles for heterogeneous NOx reduction: anomalous stability and reactivity of a core–shell nanostructure, Angew. Chem. Int. Ed. 44 (2005) 4539–4543.
[10] N. Kohler, C. Sun, A. Fichtenholtz, J. Gunn, C. Fang, M. Zhang, Methotrexate-immobilized poly(ethylene glycol) magnetic nanoparticles for MR imaging and drug delivery, Small 2 (2006) 785–792.
[11] M.I. Shukoor, F. Natalio, M.N. Tahir, V. Ksenofontov, H.A. Therese, P. Theato, H.C. Schröder, W.E.G. Müller, W. Tremel, Superparamagnetic γ-Fe_2O_3 nanoparticles with tailored functionality for protein separation, Chem. Commun. (2007) 4677–4679.
[12] A. Ito, M. Shinkai, H. Honda, T. Kobayashi, Medical application of functionalized magnetic nanoparticles, J. Biosci. Bioeng. 100 (2005) 1–11.
[13] H. Gu, P.L. Ho, K.W.T. Tsang, L. Wang, B. Xu, Using biofunctional magnetic nanoparticles to capture Vancomycin-resistant Enterococci and other Gram-positive bacteria at ultralow concentration, J. Am. Chem. Soc. 125 (2003) 15702–15703.
[14] D.K. Kim, M. Mikhaylova, F.H. Wang, J. Kehr, B. Bjelke, Y. Zhang, T. Tsakalakos, M. Muhammed, Starch-coated superparamagnetic nanoparticles as MR contrast agents, Chem. Mater. 15 (2003) 4343–4351.
[15] S.H. Sun, C.B. Murray, D. Weller, L. Folks, A. Moser, Monodisperse FePt nanoparticles and ferromagnetic FePt nanocrystal superlattices, Science 287 (2000) 1989–1992.
[16] S.H. Huang, M.H. Liao, D.H. Chen, Fast and efficient recovery of lipase by polyacrylic acid-coated magnetic nano-adsorbent with high activity retention, Sep. Purif. Technol. 51 (2006) 113–117.
[17] C. Xu, K. Xu, H. Gu, X. Zhong, Z. Guo, R. Zheng, X. Zhang, B. Xu, Nitrilotriacetic acid-modified magnetic nanoparticles as a general agent to bind histidine-tagged proteins, J. Am. Chem. Soc. 126 (2004) 3392–3393.
[18] Y.C. Chang, D.H. Chen, Preparation and adsorption properties of monodisperse chitosan-bound Fe_3O_4 magnetic nanoparticles for removal of Cu(II) ions, J. Colloid Interface Sci. 283 (2005) 446–451.
[19] Y.C. Chang, D.H. Chen, Recovery of gold(III) ions by a chitosan-coated magnetic nano-adsorbent, Gold Bull. 39 (3) (2006) 98–102.
[20] H. Lee, M.K. Yu, S. Park, S. Moon, J.J. Min, Y.Y. Jeong, H.W. Kang, S. Jon, Thermally cross-linked superparamagnetic iron oxide nanoparticles: synthesis and application as a dual imaging probe for cancer in vivo, J. Am. Chem. Soc. 129 (2007) 12739–12745.
[21] S.Y. Mak, D.H. Chen, Fast adsorption of methylene blue on polyacrylic acid-bound iron oxide magnetic nanoparticles, Dyes Pigments 61 (2004) 93–98.
[22] S.Y. Mak, D.H. Chen, Binding and sulfonation of poly(acrylic acid) on iron oxide nanoparticles: a novel, magnetic, strong acid cation nano-adsorbent, Macromol. Rapid Commun. 26 (2005) 1567–1571.
[23] S. Samal, R.R. Das, R.K. Dey, S. Acharya, Chelating resins VI: chelating resins of formaldehyde condensed phenolic Schiff bases derived from 4,4′-diaminodiphenyl ether with hydroxybenzaldehydes-synthesis, characterization, and metal ion adsorption studies, J. Appl. Polym. Sci. 77 (2000) 967–981.
[24] F. Rashchi, J.A. Finch, C. Sui, Action of DETA, dextrin and carbonate on lead-contaminated sphalerite, Colloids Surf. A: Physicochem. Eng. Aspects 245 (2004) 21–27.
[25] R. Qu, C. Wang, C. Ji, C. Sun, X. Sun, G. Cheng, Preparation, characterization, and metal binding behavior of novel chelating resins containing sulfur and polyamine, J. Appl. Polym. Sci. 95 (2005) 1558–1656.
[26] W.S.W. Ngah, C.S. Endud, R. Mayanar, Removal of copper(II) ions from aqueous solution onto chitosan and cross-linked chitosan beads, Funct. Polym. 50 (2002) 181–190.
[27] N. Li, R. Bai, Copper adsorption on chitosan–cellulose hydrogel beads: behaviors and mechanisms, Sep. Purif. Technol. 42 (2005) 237–247.
[28] S.S. Banerjee, D.H. Chen, Fast removal of copper ions by gum arabic modified magnetic nano-adsorbent, J. Hazard. Mater. 147 (2007) 792–799.
[29] G. Bayramoğlu, M.Y. Arıca, Ethylenediamine grafted poly(glycidylmethacrylate-co-methylmethacrylate) adsorbent for removal of chromate anions, Sep. Purif. Technol. 45 (2005) 192–199.